Stereoselectivity toward VX Is Determined by Interactions with Residues of the Acyl Pocket as Well as of the Peripheral Anionic Site of AChE†

Arie Ordentlich,‡ Dov Barak,§ Gali Sod-Moriah,§ Dana Kaplan,‡ Dana Mizrahi,§ Yoffi Segall,§ Chanoch Kronman,‡ Yishai Karton,§ Arie Lazar,|| Dino Marcus,|| Baruch Velan,‡ and Avigdor Shafferman*,‡

Departments of Biochemistry and Molecular Genetics, Organic Chemistry, and Biotechnology, Israel Institute for Biological Research, Ness-Ziona, 74100 Israel

Received May 5, 2004; Revised Manuscript Received June 22, 2004

ABSTRACT: The origins of human acetylcholinesterase (HuAChE) reactivity toward the lethal chemical warfare agent *O*-ethyl *S*-[2-(diisopropylamino)ethyl] methylphosphonothioate (VX) and its stereoselectivity toward the P^S-VX enantiomer (VX^S) were investigated by examining the reactivity of HuAChE and its mutant derivatives toward purified enantiomers of VX and its noncharged isostere *O*-ethyl *S*-(3-isopropyl-4-methylpentyl) methylphosphonothioate (nc-VX) as well as echothiophate and its noncharged analogue. Reactivity of wild-type HuAChE toward VX^S was 115-fold higher than that toward VX^R, with bimolecular rate constants of 1.4×10^8 and 1.2×10^6 min^{-1} M^{-1}. HuAChE was also 12500-fold more reactive toward VX^S than toward nc-VX^S. Substitution of the cation binding subsite residue Trp86 with alanine resulted in a 3 order of magnitude decrease in HuAChE reactivity toward both VX enantiomers, while this replacement had an only marginal effect on the reactivity toward the enantiomers of nc-VX and the noncharged echothiophate. These results attest to the critical role played by Trp86 in accommodating the charged moieties of both VX enantiomers. A marked decrease in stereoselectivity toward VX^S was observed following replacements of Phe295 at the acyl pocket (F295A and F295A/F297A). Replacement of the peripheral anionic site (PAS) residue Asp74 with asparagine (D74N) practically abolished stereoselectivity toward VX^S (130-fold decrease), while a substitution which retains the negative charge at position 74 (D74E) had no effect. The results from kinetic studies and molecular simulations suggest that the differential reactivity toward the VX enantiomers is mainly a result of a different interaction of the charged leaving group with Asp74.

The catalytic efficiency of acetylcholinesterase (AChE,[1] EC 3.1.1.7) and its high reactivity toward both covalent and noncovalent inhibitors are believed to originate from the unique architecture of the AChE active center (*1*−*3*). Elements of this architecture, unraveled during over a decade by X-ray crystallography (*4*−*7*), site-directed mutagenesis, and kinetic studies of the AChE mutants (*8*−*15*), include (a) the esteratic site containing the active site serine, (b) the "oxyanion hole" consisting of residues Gly120(118), Gly121-(119), and Ala204(201), (c) the "anionic subsite" or the choline binding subsite [Trp86(84)], (d) the hydrophobic site for the alkoxy leaving group of the substrate containing an "aromatic patch" that includes residues Trp86(84), Tyr337-(330), and Phe338(331), (e) the acyl pocket [Phe295(288) and Phe297(290)], and (f) the peripheral anionic site (PAS) localized at or near the rim of the active site gorge and consisting of residues Asp74(72), Tyr72(70), Tyr124(121), Trp286(279), and Tyr341(334). Among the AChE ligands which have been used to probe the molecular environment of the active center, organophosphorus (OP) inhibitors, such as dialkyl phosphates and methylphosphonates, are particularly suitable. Their unusually high reactivity toward the enzyme indicates efficient accommodation by the active center binding elements (*16*−*20*). The high affinity toward OP inhibitors may result from their ground-state tetrahedral geometry that mimics to some degree the spatial disposition of the intermediate ACh−AChE adduct (*16*, *19*). In the noncovalent OP−AChE complex, accommodation of the tetrahedral phosphoryl moiety includes polar interactions of the phosphyl oxygen with the oxyanion hole as well as that of His447 with the phosphate (or phosphonate) alkoxy oxygen. The alkyl moieties of the inhibitor are contained

† This work was supported by the U.S. Army Research and Development Command, Contracts DAMD17-00-C-0021 and DAMD17-03-C-0012 (to A.S.).

* To whom correspondence should be addressed: IIBR, Ness-Ziona, 74100 Israel. Telephone: (972)-8-9381595. Fax: (972)-8-9401404. E-mail: avigdor@iibr.gov.il.

‡ Department of Biochemistry and Molecular Genetics.

§ Department of Organic Chemistry.

|| Department of Biotechnology.

[1] Abbreviations: ACh, acetylcholine; AChE, acetylcholinesterase; ATC, acetylthiocholine; BChE, butyrylcholinesterase; BCh, butyrylcholine; ChE, cholinesterase; DEFP, diethyl phosphorofluoridate; DFP, diisopropyl phosphorofluoridate; echothiophate, *O*,*O*-diethyl *S*-(2-ethyl)-trimethylammonium phosphorothioate iodide; nc-echothiophate, *O*,*O*-diethyl *S*-(3,3-dimethylbutyl)phosphorothioate; HuAChE, human acetylcholinesterase; MEPQ, 7-(methylethoxyphosphinyloxy)-1-methylquinolinium iodide; soman, 1,2,2-trimethylpropyl methylphosphonofluoridate; TcAChE, *Torpedo californica* acetylcholinesterase; TMTFA, *m*-(*N*,*N*,*N*-trimethylammonio)trifluoroacetophenone; VX, *O*-ethyl *S*-[2-(diisopropylamino)ethyl] methylphosphonothioate; nc-VX, *O*-ethyl *S*-(3-isopropyl-4-methylpentyl) methylphosphonothioate. Amino acids and numbers refer to HuAChE, and the numbers in parentheses refer to the positions of analogous residues in TcAChE according to the recommended nomenclature (*50*).

10.1021/bi0490946 CCC: $27.50
Published on Web 08/11/2004

within the hydrophobic domains of the active center (acyl pocket and the hydrophobic patch), with the spatial differences between those sites presumably contributing to the inherent asymmetry of the AChE active center environment (*17*). The resulting stereoselectivity in particular with respect to methylphosphonofluoridates was utilized for in-depth investigation of the hydrophobic and steric interactions with the structural elements of the active center (*17*). Early modeling studies attributed the 10^4-fold stereoselectivity of AChE toward the P^S-enantiomer of sarin mainly to the restrictive dimensions of the acyl pocket (*21*). More recent studies with the diastereomers of soman suggest that a more complex array of interactions is affecting affinity and reactivity in the corresponding phosphorylation reactions (*17*). In the case of phosphonofluoridates, those interactions do not seem to include the leaving group, and therefore, interactions with the fluorine do not contribute to AChE stereoselectivity toward soman.

Interaction of the AChE active center with OP agents bearing a positively charged leaving group is characterized by additional polar interaction that should affect the affinity as well as the stereoselectivity toward these inhibitors (*20*, *22*, *23*). Indeed, AChE inhibition studies with various charged and noncharged *O*-ethyl methylphosphonothioates demonstrated the contribution of such polar interactions to the reactivities of the respective inhibitors (*24*). All those reactions result in the same phosphonylation product (*O*-ethyl methylphosphono-AChE), the structure of which has recently been determined by X-ray crystallography, following AChE phosphonylation by VX (*25*). Also, AChE stereoselectivity toward certain *O*-alkyl *S*-[(trimethylamino)ethyl] methylphosphonothioates was found to be much lower than that found for analogous phosphonofluoridates (*20*, *23*). These studies indicated also that the thiocholine leaving group of these inhibitors is oriented toward the gorge entrance and that residue Asp74 is a primary determinant in AChE specificity for cationic organophosphorus agents (*20*). This finding is quite surprising in view of the X-ray structures of AChE in complex with noncovalent inhibitors such as edrophonium (*26*) or conjugated with covalent modifiers such as TMTFA (*27*) that show invariably that the ammonium cationic head points toward the anionic subsite residue Trp86 and is quite remote from Asp74.

In this study, we investigate the origins of HuAChE stereoselectivity toward the enantiomers of VX through comparisons with their noncharged isosteres as well as with the symmetrical diethyl phosphates echothiophate and its noncharged analogue. Our results indicate that in the case of VX stereoselectivity is a result of multiple interactions involving several elements of the active center and the peripheral anionic site, including polar interactions with the charged leaving group.

MATERIALS AND METHODS

Enzymes and Reagents. Mutagenesis of AChE was performed by DNA cassette replacement into a series of HuAChE sequence variants, which conserve the wild-type coding specificity (*28*) but carry new unique restriction sites (*10*). Generation of mutants D74N, D74E, W86A, W86F, G122A, W286A, F295A, F297A, Y337A, F338A, and Y341A was described previously (*10*, *16*, *29*−*31*). The D74E mutant was introduced by replacing the *Acc*I−*Esp*I DNA fragment of the pAChE-w4 variant (*10*) with the respective synthetic DNA duplexes carrying the mutated GAG(Glu) codon.

Scheme 1[a]

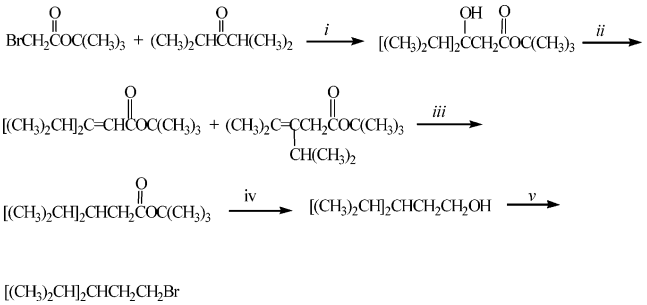

[a] (i) Zn, THF, reflux; (ii) $POCl_3$, pyridine; (iii) H_2, Pd-5%/C; (iv) $LiAlH_4$, ether, room temperature; (v) PBr_3, benzene, reflux.

Expression of recombinant HuAChE and its mutants in a human embryonal kidney-derived cell line (HEK-293) (*10*, *32*, *33*) and generation of all the mutants were described previously (*8*, *10*, *29*, *31*, *34*). Stable recombinant cell clones expressing high levels of each of the mutants were established according to the procedure described previously (*33*). Acetylthiocholine iodide (ATC) and 5,5′-dithiobis(2-nitrobenzoic acid) (DTNB) were purchased from Sigma.

Organophosphate Inhibitors. The enantiomers of VX [*O*-ethyl *S*-(2-diisopropylaminoethyl) methylphosphonothioate] were synthesized by following a literature procedure (*35*). The final reaction step was modified by using *N*,*N*-diisopropylaziridinium chloride rather than *N*,*N*-diisopropylaminoethyl chloride that gave the pure enantiomers without further purification: ^{1}H NMR ($CDCl_3$) δ 1.00 (d, J = 6.5 Hz, 12H), 1.33 (t, J = 7.0 Hz, 3H), 2.78 (m, 2H), 2.99 (septet, J = 6.4 Hz), 4.11 (m, 2H); ^{31}P{^{1}H} NMR δ 51.14; $[\alpha]^{20}_D$ = 31.0° (*R*), −30.2° (*S*).

Enantiomers of nc-VX [*O*-ethyl *S*-(3-isopropyl-4-methylpentyl) methylphosphonothioate] were synthesized from the enantiomeric *O*-ethyl methylphosphonothioate sodium salt (*36*) and 3-(2-bromoethyl)-2,4-dimethylpentane. The bromide was prepared according to Scheme 1. Detailed procedures of the synthetic steps and characterization of the intermediates are provided in the Supporting Information.

Kinetic Studies. HuAChE activity was assayed according to the method of Ellman *et al.* (*37*) in the presence of 0.1 mg/mL BSA, 0.3 mM DTNB, 50 mM sodium phosphate buffer (pH 8.0), and various concentrations of ATC at 27 °C and monitored with a Thermomax microplate reader (Molecular Devices).

Measurements of phosphorylation rates for VX and nc-VX were carried out with at least four different concentrations of VX and nc-VX (PX), and enzyme residual activity (E) at various times was monitored. The apparent bimolecular phosphorylation rate constants (k_i) determined under pseudo-first-order conditions were computed from the plot of slopes of ln(E) versus time at different inhibitor concentrations (see Scheme 2). Rate constants under second-order conditions were determined from plots of $\ln\{E/[I_o - (E_o - E)]\}$ versus time (*16*). Both VX and nc-VX were stable in the reaction medium (phosphate buffer) within the time scale of the kinetic experiments. The half-life time ($t_{1/2}$) for hydrolysis of both inhibitors was more than 100 h as determined by

Scheme 2

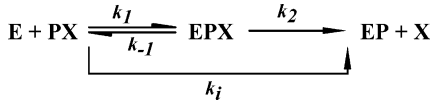

Scheme 3

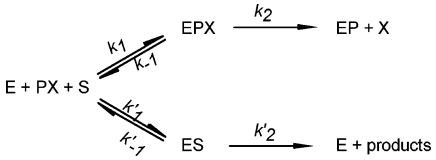

$^{31}P\{^{1}H\}$ NMR. This estimation is in accordance with measurement of VX stability at pH 8 in an aqueous solution (*38*).

Determination of the bimolecular rate constants for phosphorylation by echothiophate and nc-echothiophate was carried out following the double-reciprocal method of Hart and O'Brien (*39*), as described previously (*16*). Appart from bimolecular rate constants, this method allows for evaluation of the apparent dissociation constant for the enzyme−inhibitor Michaelis complex ($K_d = k_{-1}/k_1$) and the phosphylation rate constant of the reaction (k_2; see Scheme 3).

Molecular Dynamics Simulations. Simulations of the HuAChE Michaelis complexes with VX^S and VX^R were performed using the AMBER 5.0 suite of programs with an all atom parameter set. Characterization and visual examination of the molecular structures were carried out using the molecular modeling package SYBYL 6.7 running on an SGI Octane workstation. The starting conformation of the enzyme was obtained from the X-ray structure of the HuAChE−fasciculin complex model (*6*; Protein Data Bank entry 1b41). The rim of the active site gorge as well as the active center was solvated by adding a spherical cap of water (using the SOL option of AMBER). The cap waters were restrained by a soft half-harmonic potential to avoid evaporation without affecting the protein movement. The part of the complex included in the simulation (using the belly option in AMBER) was comprised of residues in the active center gorge and around the ligand as well as the ligand itself (~150 residues were included, and the number varied slightly depending upon the definition of the belly region for the specific simulation experiments). Partial charges of the VX enantiomers were asigned the Del Re method implemented in SYBYL. Model optimization and dynamics simulations were carried out according to a protocol described previously (*3*)

RESULTS

Preparation of Organophosphate Inhibitors. Resolved *O*-ethyl methylphosphonothioic acids, which served as starting materials for both the VX and nc-VX enantiomers (Figure 1), were synthesized following the procedure of Berman and Leonard (*36*). S-Alkylation of the resolved enantiomers, using *N*,*N*-diisopropylaziridinium chloride, yielded pure VX enantiomers. This procedure proved to be more convenient than that using *N*,*N*-diisopropylaminoethyl chloride, as reported previously (*35*). Analogous preparation of the nc-VX enantiomers was carried out using 3-(2-bromoethyl)-2,4-dimethylpentane as the alkylating agent. Preparation of this alkyl bromide was carried out in five steps

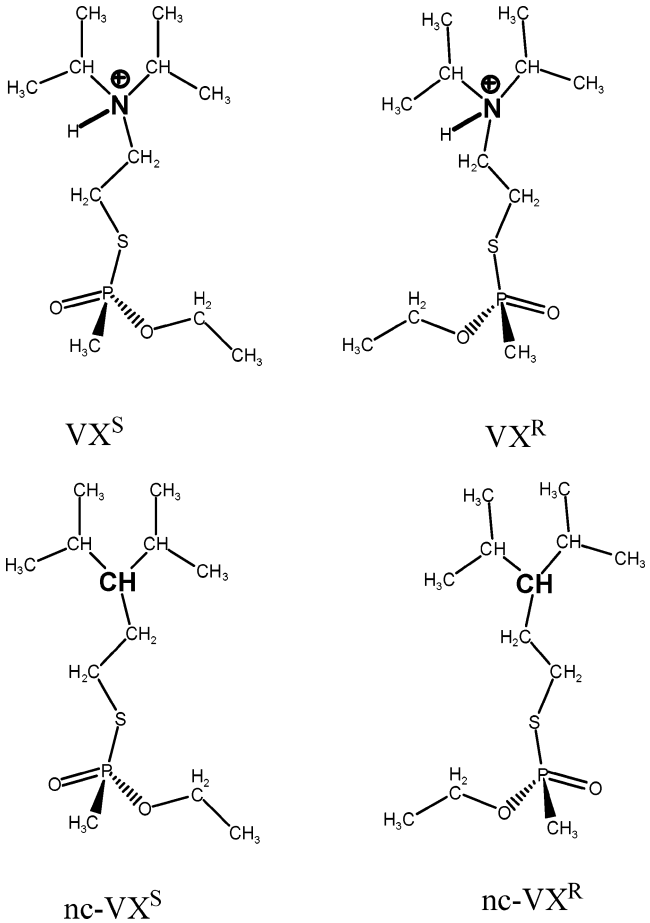

FIGURE 1: Chemical formulas of VX enantiomers and their noncharged isosteres. The protonated forms of both VX^S and VX^R are shown since the charged species are present under our experimental conditions [the pK_a value for VX was recently reported to be 9.4 (*49*)].

(see Scheme 1 and the Supporting Information), and the resulting nc-VXs were >95% enantiomerically pure as shown by ^{1}H NMR using the chiral reagent (*R*)-2,2,2-trifluoro-1-(9-anthryl)ethanol.

O,*O*-Diethyl *S*-(3,3-dimethylbutyl) phosphorothioate ("nc-echothiophate") was prepared from 3,3-dimethylbutyl bromide (*8*) and the potassium salt of diethyl thiophosphoric acid.

Reactivity of HuAChE toward VX and nc-VX Enantiomers. Reactivity of recombinant wild-type HuAChE toward VX^S was 115-fold higher than that toward VX^R, with the values of the bimolecular rate constants being 1.4×10^8 and 1.2×10^6 min^{-1} M^{-1}, respectively. Such HuAChE stereoselectivity toward VX enantiomers is consistent with earlier reports on AChE reactivities toward VX (*35*, *40*) and toward other charged methylphosphonothiocholines (*20*, *36*). In particular, AChE from bovine erythrocytes was reported to display a 200-fold stereoselectivity toward the VX^S enantiomer (*40*).

The HuAChE enzyme displayed 60-fold stereoselectivity toward the noncharged nc-VX^S (Figure 1), with reactivity toward this enantiomer being ~12500-fold lower than that toward VX^S (Tables 1 and 2). The corresponding reactivity toward the nc-VX^R was exceedingly low (the value of bimolecular rate constant k_i was 2×10^2 min^{-1} M^{-1}), and the actual measurement of this constant, as well as of those for other HuAChE enzymes, was made possible only by the

Table 1: Apparent Bimolecular Rate Constants[a] (k_i) of Phosphonylation of HuAChE Enzymes by VX^S and VX^R

	VX^S		VX^R		
HuAChE	k_i ($\times 10^{-4}$ M^{-1} min^{-1})	WT/ mutant	k_i ($\times 10^{-4}$ M^{-1} min^{-1})	WT/ mutant	VX^S/ VX^R
wild type	13700	1	118.0	1	115
F295A	1600	9	360.0	0.3	5
F297A	1560	9	22.5	5	70
F295A/F297A	18	760	3.4	35	5
W86F	465	30	10.0	12	50
W86A	3	4500	0.1	980	30
D74N	107	130	48.0	2.5	2
D74E	5900	2	31.0	4	190
W286A	13000	1	85.0	1	170
Y341A	5100	3	13.0	9	370
Y337A	4000	3	30.0	4	130
F338A	2700	5	30.0	4	90
G122A	7	2000	0.3	400	25

[a] Values represent the mean of triplicate determinations with a standard deviation not exceeding 20%.

Table 2: Apparent Bimolecular Rate Constants[a] (k_i) of Phosphonylation of HuAChE Enzymes by nc-VX^S and nc-VX^R

	nc-VX^S		nc-VX^R		
HuAChE	k_i ($\times 10^{-4}$ M^{-1} min^{-1})	WT/ mutant	k_i ($\times 10^{-4}$ M^{-1} min^{-1})	WT/ mutant	nc-VX^S/ ncVX^R
wild type	1.1	1	0.02	1	60
F295A	0.5	2	0.03	1	20
F297A	3.4	0.3	0.02	1	170
F295A/F297A	0.04	27	0.003	7	13
W86F	0.6	1.8	0.025	1	25
W86A	0.3	3.7	0.01	2	30
D74N	2.0	0.5	0.03	1	70
D74E	0.9	1	0.01	2	90
W286A	1.5	0.7	0.015	1	100
Y341A	2.5	3	0.02	1	23
Y337A	63.0	0.03	0.07	0.3	900
F338A	0.9	1	0.003	7	300
G122A	0.02	60	0.0004	50	50

[a] Values represent the mean of triplicate determinations with a standard deviation not exceeding 20%.

stability of the inhibitors in buffer solutions (see Materials and Methods) and by the ability to produce sufficient amounts of recombinant enzyme proteins, using the remarkably efficient HEK 293 expression system (*10*, *33*).

Wild-type HuAChE exhibited a 850-fold higher reactivity toward the diethyl phosphate echothiophate than toward its noncharged isostere nc-echothiophate (see Table 3). Since for both phosphates disposition of the phosphyl ethoxy substituents with respect to the HuAChE active center should be similar, the different reactivities signify the contribution of interactions with the charged leaving group. Thus, the large reactivity differences between the VX enantiomers and their corresponding noncharged isosteres (nc-VX) may have also resulted predominantly from accommodation of the diisopropylammonium group in the active center.

While interactions with the charged leaving group seem to make up the major contribution to the HuAChE affinity toward the two VX enantiomers, the question regarding the specific interactions contributing to the 115-fold stereoselectivity toward VX^S remains open. Since stereoselectivity has usually been associated with perturbations at the acyl pocket (*8*, *17*, *21*), the lower reactivity of HuAChE toward VX^R may still be a result of inferior accommodation of the ethoxy substituent. Comparison of the bimolecular rate constant (k_i) for HuAChE phosphonylation by VX^R and by echothiophate shows quite similar values (1.2×10^6 and 1.5×10^6 min^{-1} M^{-1}, respectively), suggesting that such interactions of the ethoxy moiety may indeed determine the affinities of these two charged organophosphorus inhibitors. On the other hand, HuAChE reactivity toward nc-echothiophate was found to be only 6-fold lower than toward nc-VX^S, indicating that replacement of a methyl group with an ethoxy group in the acyl pocket results in a roughly 6-fold decrease in binding affinity. This effect seems to be too small to account for the observed HuAChE stereoselectivity toward VX^S.

Therefore, it was important to investigate the dependence of stereoselectivity toward VX enantiomers on interactions with the different components of the active center functional architecture. To this end, enzyme derivatives with modifications introduced by site-directed mutagenesis at active center subsites involved in ligand accommodation such as the acyl pocket, anionic subsite, hydrophobic subsite, peripheral anionic site, and the loop of the oxyanion hole were introduced. Kinetic evaluation of the reactivity characteristics of these HuAChE enzymes toward the charged and noncharged VX as well as toward the symmetric phosphate echothiophate allowed for characterization of the main elements of the HuAChE chirality toward charged methylphosphonates.

Stereoselectivity of HuAChE Enzymes Carrying Mutations at the Acyl Pocket. Replacements of acyl pocket residues Phe295 or Phe297 with alanine had quite different effects on stereoselectivity toward the VX^S enantiomer. While the F295A enzyme was only 5-fold more reactive toward the VX^S than toward the VX^R enantiomer, the corresponding ratio for the F297A was 70-fold, resembling that of wild-type HuAChE (see Table 1). The decrease in stereoselectivity of the F295A enzyme resulted mainly from its lower reactivity toward VX^S (9-fold) rather than from an increased reactivity toward VX^R (3-fold; see Table 1). Thus, while structural perturbation at position 295 of the acyl pocket affects stereoselectivity toward the VX^S enantiomer, the basis for the differential reactivity does not seem to involve steric exclusion from the acyl pocket. The notion that steric congestion at the acyl pocket does not determine HuAChE stereoselectivity toward VX^S is also supported by reactivities of the F297A enzyme toward the VX enantiomers. In this case, the mutated enzyme is less reactive toward both VX^S (9-fold) and VX^R (5-fold), suggesting a suboptimal accommodation of the phosphonate in the active center irrespective of the substituent adjacent to the acyl pocket.

Mutations at positions 295 and 297 in HuAChE had an only small effect on the reactivity of the corresponding enzymes toward the nc-VX enantiomers (all effects were within a factor of 3; see Table 2). These findings seem to suggest that there is nearly no energetic penalty for accommodating the nc-VX^R ethoxy substituent in the HuAChE acyl pocket.

Replacement of the aromatic residue at position 295 resulted in a 40-fold reactivity increase toward the diethyl phosphate, echothiophate, relative to the wild-type enzyme. The corresponding replacement at position 297 had practically no effect, suggesting that the orientation of the ethoxy group with respect to the acyl pocket in the echothiophate−

Table 3: Apparent Bimolecular Rate Constants[a] (k_i) of Phosphonylation of HuAChE Enzymes by Echothiophate and nc-Echothiophate

	echothiophate			nc-echothiophate		
HuAChE	k_i ($\times 10^{-4}$ M^{-1} min^{-1})	k_2 (min^{-1})	K_i ($\times 10^6$ M)	k_i ($\times 10^{-4}$ M^{-1} min^{-1})	k_2 (min^{-1})	K_i ($\times 10^6$ M)
wild type	154	3.7	2.4	0.18	0.6	325
F295A	6000	0.8	0.013	1.46	0.95	65
F297A	58	4.4	7.6	0.2	0.3	146
F295A/F297A	45	ND[b]	ND[b]	0.02	ND[b]	ND[b]
W86F	17	0.7	4.2	0.25	0.56	220
W86A	0.08	0.8	1020	0.02	0.8	4570
D74N	3.8	5.5	147	0.96	0.55	57
D74E	32	1.1	3.4	0.18	0.92	510
D74G	14	0.9	3.2	0.72	0.6	83
W286A	260	1.7	0.64	1.07	0.6	55
Y341A	40	1.2	3.0	0.4	0.97	244
Y337A	34	1.8	5.5	0.06	0.34	540
F338A	12	1.7	14.1	0.009	0.13	1500

[a] Values represent the mean of triplicate determinations with a standard deviation not exceeding 20%. [b] Not determined.

HuAChE complex is somewhat different from that of the corresponding complex with the VX^R enantiomer. This different reactivity toward echothiophate may be related to the other ethoxy substituent since similar effects, due to mutations at the acyl pocket, were reported for neutral diethyl phosphates such as DEFP and paraoxon (*16*).

The double mutant F295A/F297A exhibits a lower affinity for both VX and nc-VX, with consistently larger effects for the P^S-enantiomers (see Tables 1 and 2). Interestingly, the reactivity decline toward VX^S is much more pronounced than that toward nc-VX^S (760- and 27-fold, respectively), suggesting that the reactivity decrease does not seem to be a result of deficient accommodation of the methyl group. It appears also that the outcome of removing aromatic moieties from the acyl pocket (e.g., enhanced mobility of the catalytic His447; see refs *1*−*3*) has a stronger effect on the presumably more rigidly oriented VX^S within the Michaelis complex than on the neutral nc-VX^S.

Stereoselectivity of HuAChE Enzymes Carrying Mutations at the Anionic Subsite, the Choline Binding Site. Replacement of Typ86 with alanine had a dramatic effect on the reactivity toward both VX enantiomers, yet only a minor effect on stereoselectivity toward VX^S (Table 1). The decrease of the W86A HuAChE reactivity toward the VX^S and VX^R enantiomers as compared to the reactivity toward the wild-type enzyme (the values of bimolecular rate constants decreased by 4500- and ∼1000-fold, respectively; see Table 1) was compatible with what was observed in the past for other covalent or noncovalent charged ligands (*8*, *14*, *24*, *25*, *29*, *30*). The corresponding effects of the replacement of Trp86 with phenylalanine were much weaker and consistent with the well-established role of the aromatic residue at position 86 as the main interaction locus of the charged moieties of AChE ligands (*14*, *30*). Similarly, W86A was 1925-fold less reactive toward echothiophate than the wild-type enzyme (Table 3). These effects are considerably stronger than those reported for interaction of similarly charged methylphosphonates, P^S-*O*-cycloheptyl methylphosphonylthiocholine (40-fold), or the corresponding P^R-enantiomer (33-fold) with the W86A mutant of mouse AChE (*20*).

Mutations at the anionic subsite had only minor effects on HuAChE affinities toward the nc-VX enantiomers and the nc-echothiophate (Tables 2 and 3), demonstrating again that the role of the aromatic moiety at position 86 consists mainly of accommodating the charged moieties of substrates and other charged ligands. However, reactivity of W86A HuAChE toward nc-VX^S was still 10-fold lower than that toward VX^S, suggesting participation of other elements in the active center to accommodate the charged leaving group. Similarly, reactivity of this enzyme toward nc-echothiophate was 4 times lower than that toward echothiophate (Table 3).

Stereoselectivity of HuAChE Enzymes Carrying Mutations at the Hydrophobic Subsite. Stereoselectivity toward VX^S as well as reactivity toward both VX enantiomers is only slightly affected by single replacements of elements of the hydrophobic pocket [aromatic patch (*14*)], residues Tyr337 and Phe338 (Table 1). The effects are weak (∼4-fold) and do not indicate disruption of major interactions with the active center environment. In view of this result, it was rather surprising to find that replacement of this residue with alanine resulted in a 57-fold increase in affinity toward nc-VX^S, suggesting that the *S*-alkyl leaving group of nc-VX^S appears to interfere with the aromatic moiety of Tyr337 (Table 2). A small increase in affinity is observed also for nc-VX^R, and consequently, the stereoselectivity of this enzyme toward nc-VX^S was 900-fold. Such an effect on stereoselectivity due to replacement of Tyr337 indicates that the leaving groups in VX and in nc-VX may point to somewhat different regions of the active site. Furthermore, Y337A HuAChE was only 3-fold less reactive toward the nc-echothiophate than the wild-type enzyme (Table 3), implying that the orientation of its leaving group, in the nc-echothiophate−Y337A complex, resembles more that of nc-VX^R than that of VX^S (see Table 2). The findings indicate also that the positively charged leaving groups of either the VX enantiomers or echothiophate do not interact with the aromatic moiety of Tyr337 (Tables 1 and 3). In this respect, the findings are consistent with our previously reported conclusion that residue Tyr337 is not a part of the anionic subsite participating in accommodation of the cationic headgroups of AChE ligands (*14*), as suggested previously (*27*, *41*).

Stereoselectivity of HuAChE Enzymes Carrying Mutations at the Peripheral Anionic Site (PAS). Replacement of Asp74 with asparagine practically abolished stereoselectivity toward the VX^S enantiomer. D74N HuAChE was 130-fold less reactive toward VX^S, while its reactivity toward VX^R resembled that of the wild-type enzyme (see Table 1). In

contrast, substitution of the aspartate at position 74 with another acidic residue, glutamate, yielded an enzyme with affinities toward both VX enantiomers nearly the same as those of wild-type HuAChE. These results show that VX^S interacts with the acidic residue at position 74 of HuAChE, suggestng that in the case of VX enantiomers charged interactions of the leaving group are a major determinant of stereoselectivity. Thus, it is reasonable to expect that the charged leaving groups in the HuAChE Michaelis complexes of VX^S and VX^R assume somewhat different orientations, with the cationic head in the VX^S complex closer to the Asp74 carboxylate than in the corresponding VX^R complex.

Reactivity of the D74N HuAChE toward echothiophate was also 40-fold lower than that of the wild-type enzyme (see Table 3), yet in this case, the decrease may not result from loss of a specific electrostatic interaction of the cationic leaving group. This notion is suggested by the similar effects of replacing residue Asp74 with glutamic acid or with the noncharged residue glycine (5- and 10-fold respectively; see Table 3 and ref *22*).

Replacement of Asp74 with asparagine had practically no effect on the reactivity toward nc-VX enantiomers (see Table 2). In addition, a minor (4−5-fold) increase was observed in the activity of D74N and D74G HuAChEs toward nc-echothiophate (Table 3). These findings are consistent with our previous observation that residue Asp74 contributes predominantly to binding of charged ligands in the HuAChE active center (*22*, *29*).

Replacement of other components of the PAS, Tyr341 and Trp286, had an only limited effect on reactivity toward VX enantiomers. The most pronounced effect was that on reactivity toward VX^R due to substitution of position 341 with alanine (9-fold). Also, these replacements had nearly no effect on affinities toward nc-VX enantiomers or nc-echothiophate (see Tables 1−3).

Stereoselectivity of HuAChE Carrying a Mutation at Position 122 Next to the Oxyanion Hole. Residue Gly122 is adjacent to oxyanion hole residues Gly120 and Gly121. Replacement of Gly122 with alanine was shown to introduce a methyl group into the space of the acyl pocket (*15*; see also ref *27*). As already reported, the reactivity of G122A toward phosphonates is affected to a larger extent than that toward phosphates (*15*), due to the size of the moiety in the immediate vicinity of the Ala122 methyl group [e.g., for DEFP reactivity of G122A HuAChE was 95-fold lower than for wild-type HuAChE, and for soman the corresponding ratio was 500 (*15*)]. In the case of VX^S, G122A HuAChE was 2000-fold less reactive than the wild-type enzyme, while for VX^R, the corresponding ratio is 400 (Table 1). Thus, G122A HuAChE displayed lower stereoselectivity, than the wild-type enzyme, toward the VX^S enantiomer (25-fold), probably due to impaired accommodation of the phosphonyl methyl group in the acyl pocket as a consequence of replacement of the hydrogen with a methyl group in the G122A mutant. The G122A enzyme was also 260-fold less reactive toward echothiophate than wild-type HuAChE ($k_i = 6 \times 10^3\ M^{-1}\ min^{-1}$), suggesting that in the phosphate−G122A adduct the phosphate ethoxy group may be positioned in the acyl pocket more like that of VX^R (see Table 1) than like that of the homologous phosphate DEFP (*15*). These observations may indicate that in the Michaelis complexes of both VX enantiomers or of echothiophate the methyl and the ethoxy moieties are located closer to Ala122 than in the corresponding complexes of DEFP or soman. Such proximity, which may be induced by the rigid orientation of the charged leaving group, suggests also that the corresponding phosphyl moieties are positioned close to the oxyanion hole.

The reactivity of G122A HuAChE toward the nc-VX^S enantiomer was 60-fold lower than that of the wild-type enzyme (see Table 2). Such a reactivity decrease is much smaller than what could be expected from comparison to the corresponding ratios for both VX^S and soman (2000- and 500-fold, respectively), again suggesting that accommodation of nc-VX^S in the HuAChE active center is quite different from that of the other phosphonates.

Molecular Modeling of Michaelis Complexes of HuAChE with VX Enantiomers. The question of AChE stereoselectivity toward VX^S has already been addressed in the past by molecular dynamics simulations of the TcAChE−VX Michaelis complexes (*42*). In construction of the initial structures, it was assumed that the cationic leaving group in both the VX^S and the VX^R complexes was oriented toward the peripheral anionic site and that the electrostatic interaction with Asp72 (Asp74 in HuAChE) contributes substantially to the accommodation of the charged diisopropylammonio moiety (*20*). Such an assumption was consistent with the role played by residue Asp72 in accommodating the charged groups of certain methylphosphonothiocholines in the Michaelis complexes with TcAChE (*20*). The simulations suggested that TcAChE stereoselectivity toward VX enantiomers resulted from impaired interaction of VX^R with the oxyanion hole subsite (*42*). Our results, from kinetic studies with the wild-type and G122A enzymes, suggest, however, that in HuAChE both VX enantiomers appear to be well accommodated in the oxyanion hole. Furthermore, interactions with the oxyanion hole seem to be crucial for HuAChE reactivity toward phosphate inhibitors, and therefore, a significant misalignment of the P═O moiety with respect to this subsite could abolish the phosphorylation process (*15*). Thus, it was interesting to examine the dynamic behavior of the HuAChE−VX complexes, especially in view of the finding, from kinetic studies, regarding the role of residue Asp74 in determining HuAChE stereoselectivity toward VX (Table 1).

In this study, molecular simulations of the HuAChE−VX complexes were performed assuming that the proper orientation and proximity of the phosphorus atom with respect to O^γ of Ser203 are essential for the phosphylation process and therefore should be kept throughout the simulation. In addition, interaction distances from the phosphonyl oxygen to the oxyanion hole elements were maintained since polarization of the P═O bond was found to be crucially important to the subsequent chemical process. Therefore, during optimization of the initial structures and the dynamic simulation runs, the positioning of the VX P═O moieties was restrained with respect to the HuAChE active center. In the two diastereomeric initial structures of the VX−HuAChE Michaelis complexes, the protonated diisopropylammonio group was juxtaposed with the anionic subsite Trp86 (see Table 4). Simulation experiments showed that for the VX^R complex there was no significant change in the positioning of the cationic head with respect to residues Trp86 and Asp74 (Figure 2B). On the other hand, in the VX^S complex there is motion of the cationic head toward the gorge exit, shortening its distance from residue Asp74 (see panels A

Table 4: Changes of Relevant Distances in the HuAChE Michaelis Complexes of VX^S and VX^R following a Molecular Dynamics Simulation

	initial structures (Å)		changes in average simulated structures (ΔÅ)	
distance	VX^S	VX^R	VX^S	VX^R
$N_{G120}-O(=P)_{VX}$	2.97	2.98	0.12	0.22
$N_{G121}-O(=P)_{VX}$	2.88	3.18	−0.06	−0.21
$N_{A204}-O(=P)_{VX}$	3.40	3.10	0.27	0.10
$O^{\gamma}{}_{S203}-P_{VX}$	3.33	3.34	−0.03	0.16
$O^{\delta 1}{}_{D74}-N_{VX}$	7.30	7.69	−1.10	0.41
$C^{\delta 2}{}_{W86}-N_{VX}$	5.10	5.22	1.18	0.15

and C of Figure 2). Examination of the structures along the simulation trajectories suggested that orientation of the cationic leaving group was influenced by its interaction with the phosphonyl substituent pointing toward the acyl pocket. In the VX^S complex, the phosphonyl methyl group is accommodated in the acyl pocket, permitting the cationic leaving group to point toward the gorge entrance and to interact with both Trp86 and Asp74 (Figure 2A). On the other hand, in the VX^R complex, the ethoxy group is forced to point upward by the restricted space of the acyl pocket (see Figure 2B). Such a conformation of the ethoxy moiety interferes with the cationic leaving group, inducing an alternative conformation where the diisopropylammonio group is displaced from residue Asp74 (and toward residue Trp86), as compared to its orientation in the VX^S complex.

DISCUSSION

Early hypotheses (*43*) and modeling experiments (*21*) related the pronounced stereoselectivity of AChE toward methylphosphonofluoridates such as sarin or soman to the structure of the acyl pocket. The main reason for this assessment was that the homologous enzyme butyrylcholinesterase (BChE), in which residues at positions 295 and 297 are isoleucine and valine, respectively (*44*), was found to be more reactive than AChE toward bulky substrates such as butyrylcholine (BCh) and organophosphorus inhibitors such as diisopropyl phosphorofluoridate (DFP) but not stereoselective toward sarin (*8*, *11*, *17*, *19*, *45*). Indeed, studies of HuAChE reactivity using site-directed mutagenesis and enzyme kinetics suggested that acyl pocket residues Phe295 and to a lesser extent Phe297 determine the specificity toward acylating (substrates) and phosphorylating agents (*8*, *16*) mainly by limiting the volume of the acyl pocket. A more recent examination of stereoselectivity in reactions of HuAChE active center mutants with diastereomers of soman suggested that while the AChE acyl pocket is in fact the main determinant of the relative reactivity toward the P^S- and the P^R-diastereomers, the actual mechanism of stereoselectivity is only partially related to steric interference (*17*). Further inquiry into the consequences of structural modifications at the HuAChE acyl pocket led us to propose that residues Phe295 and Phe297 are also part of an aromatic system involved in "trapping" the catalytic His447 (*1*, *2*). Thus, modifications of the AChE acyl pocket may perturb the positioning of His447 and thereby impair the accommodation of tetrahedral species in the active center. Such modifications of the acyl pocket could be brought about either by accommodation of bulky groups, leading to a significant relocation of the side chains of both Phe295 and Phe297, or by replacement of these residues with aliphatic amino acids (*1*−*3*).

Structural characteristics of the acyl pocket also seem to play a role in determining HuAChE stereoselectivity toward VX^S, as demonstrated by the mere 5-fold stereoselectivity of the F295A and F295A/F297A enzymes (see Table 1). For the latter, the 760-fold decrease in the reactivity toward the VX^S enantiomer was accompanied by an only 35-fold decrease toward VX^R. Apparently, the overall effect of the double mutation at the acyl pocket, on reactivity toward VX^R, was smaller due to some compensating factor. Such compensation could come from relief of steric pressure (due to removal of the bulky aromatic residues) on the ethoxy substituent in the acyl pocket, yet there is no evidence that accommodation of an ethoxy group results in perturbation of the acyl pocket. In fact, the lack of AChE stereoselectivity toward MEPQ (see Figure 3), where all the phosphorus substituents apart from the charged leaving group are identical to those of VX (*46*), indicates that the acyl pocket accommodates equally well the methyl and ethoxy substituents. Therefore, the different effects, due to modifications of the acyl pocket, on reactivity toward the VX^S and VX^R enantiomers must originate from interactions with other elements of the active center. Indeed, for both the VX^S and VX^R enantiomers, interactions of the charged leaving group appear to be another major determinant of HuAChE stereoselectivity. The findings that D74N HuAChE was practically devoid of stereoselectivity toward VX^S, and yet reactivity of this mutant toward VX^R was nearly equivalent to that of the wild-type enzyme, indicated that the difference in HuAChE accommodation of the two VX enantiomers can be reduced to a single interaction of the charged phosphonyl substituent with Asp74. Thus, while the diisopropylammonium moiety in Michaelis complexes of both VX^S and VX^R enantiomers interacts mainly with the anionic subsite residue Trp86, as demonstrated by the respective 980- and 4500-fold decreases in reactivity toward the W86A enzyme, respectively (Table 1), in the HuAChE−VX^S complex additional stabilization is provided by its interaction with the carboxylate of residue Asp74. In fact, interaction of the thiocholine leaving groups of certain *O*-alkyl *S*-[(trimethylamino)ethyl] methylphosphonothioates with residue Asp74 has already been suggested (*20*). However, for these ligands, *both* enantiomers interacted with Asp74 and their interaction with Trp86 was less pronounced.

If stabilizing interaction of the diisopropylammonium moiety with Asp74 is possible in the VX^S Michaelis complex, why is it absent in the corresponding VX^R complex? The reason for that is suggested by the molecular simulation experiments, which show the cationic moiety of VX^S is located nearly 2 **Å** closer to the Asp74 carboxylate than the corresponding moiety of VX^R (see Table 4). Thus, the respective locations of the VX cationic moieties seem to be determined by interactions with the phosphonyl ethoxy substituent. In the HuAChE−VX^S complex, the ethoxy group, positioned in the hydrophobic pocket, allows for an apparently optimal juxtaposition of the diisopropylammonium group with respect to residues Trp86 and Asp74 (Figure 2A). On the other hand, in the HuAChE−VX^R complex, the ethoxy group emerging from the acyl pocket induces an alternative conformation of the leaving group, in which

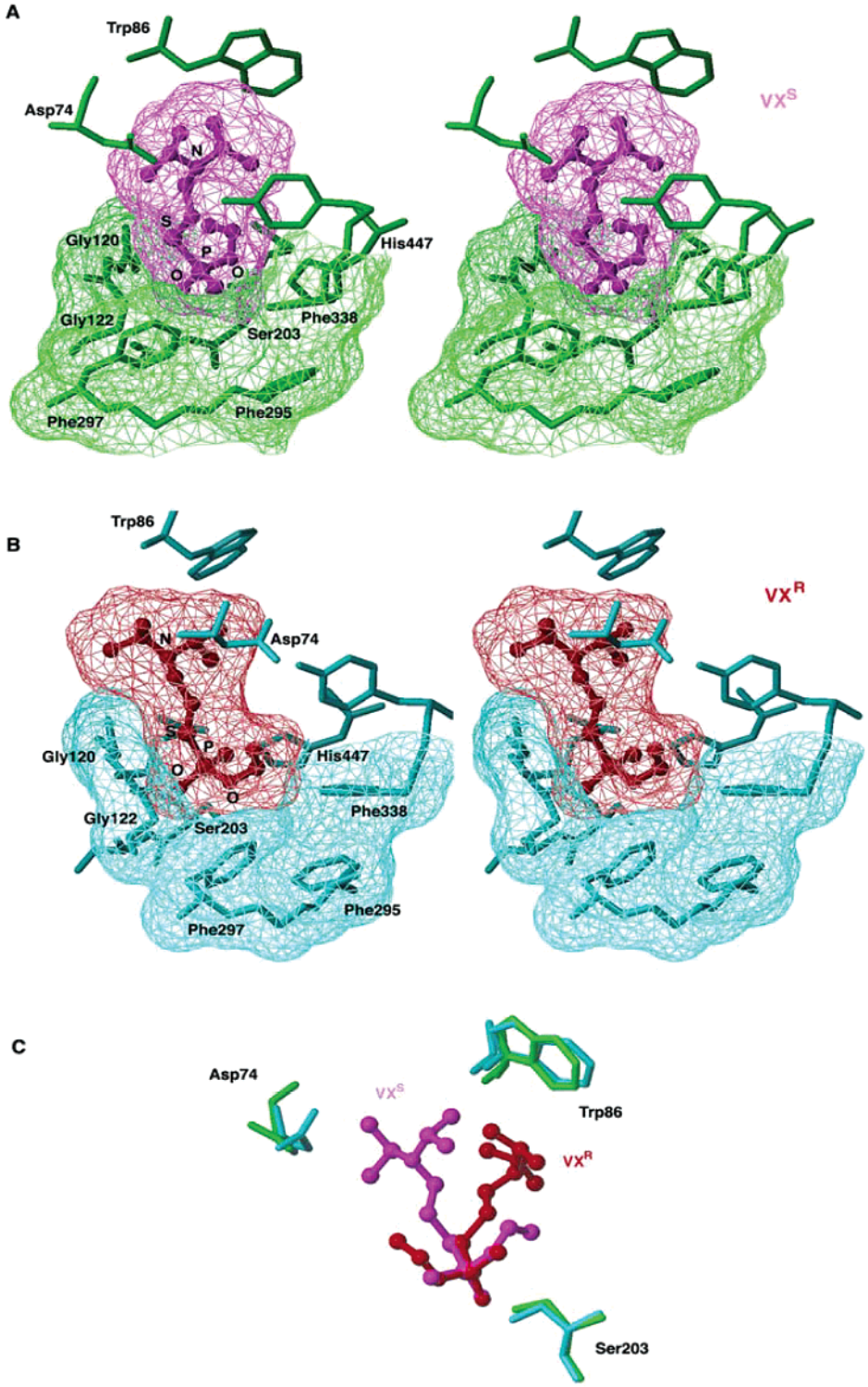

FIGURE 2: Average structures from molecular dynamics simulations of Michaelis complexes of the VX^S and VX^R enantiomers with HuAChE. Only amino acids adjacent to the inhibitor are shown, and hydrogen atoms have been omitted for clarity. Interatomic distances defining the relative orientation of the respective ligands are listed in Table 4. (A) Stereoview of the VX^S−HuAChE complex with the phosphonate depicted in magenta and the protein in green. The volumes of VX^S and the molecular environment around the acyl pocket are shown as a grid. (B) Stereoview of the VX^R−HuAChE complex with the phosphonate depicted in red and the protein in cyan. The volumes of VX^R and the molecular environment around the acyl pocket are shown as a grid. (C) Superposition of the VX^S−HuAChE and VX^R−HuAChE complex structures, using the Cα atoms of the residues shown and the respective phosphorus atoms as reference points. Note that the ammonio group of the VX^S complex (magenta) is proximal to both the Asp74 carboxylate and the indole moiety of Trp86, while that of the VX^R complex (red) points exclusively in the direction of residue Trp86.

interaction with residue Asp74 is practically precluded (Figure 2B). According to this molecular scenario, opening of the acyl pocket, as in F295A/F297A HuAChE, may relieve the steric crowding around the VX^R phosphorus, allowing for interaction of the cationic moiety in the corresponding Michaelis complex with the carboxylate of Asp74.

To our knowledge, the notion that *intramolecular* interactions of the phosphyl moiety may contribute to AChE

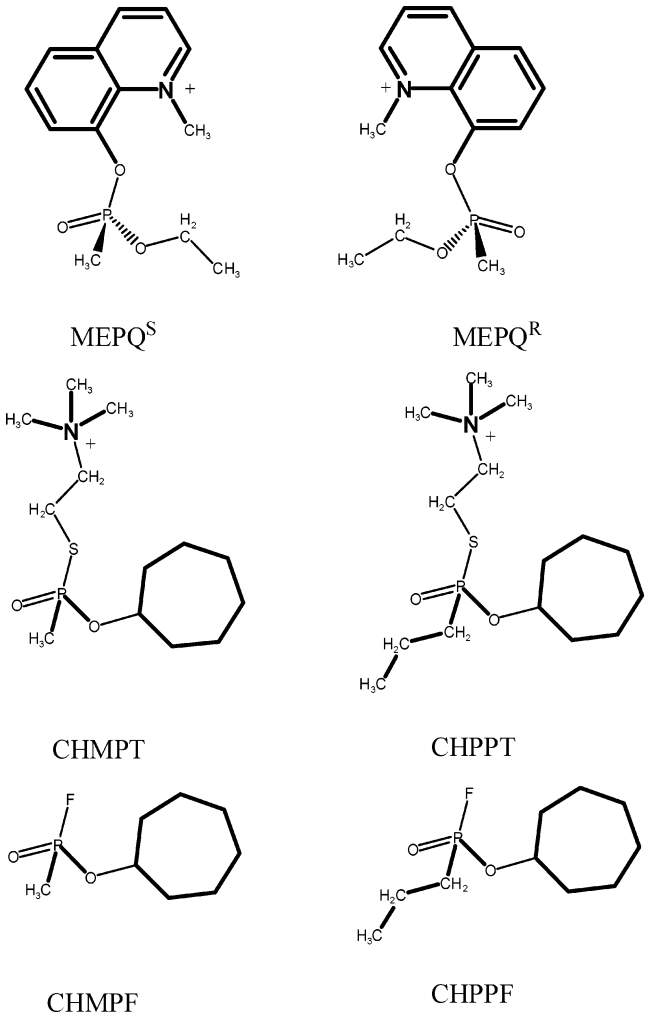

FIGURE 3: (A) Structural formulas of the MEPQ enantiomers which display nearly equivalent reactivity toward AChE (*46*) while yielding the same adducts as the corresponding enantiomers of VX. (B) Formulas of *O*-cycloheptyl alkylphosphonate AChE inhibitors bearing thiocholine and fluorine as leaving groups (*47*). Note that while reactivities of the two methyl phosphonates CHMPT and CHMPF are similar, the reactivity of CHPPT is much lower than that of CHPPF (see ref *47* and the text).

stereoselectivity toward VX^S or any other organophosphate inhibitor was not considered before. Yet certain results reported in the past seem to be consistent with the suggestion that interactions of charged leaving groups with other bulky substituents affect the inhibition properties of the corresponding phosphates and phosphonates. One such example is the different accommodation, by AChE, of *n*-propylphosphonates bearing either fluorine or thiocholine as a leaving group (*47*), as compared to the respective methylphosphonates (see Figure 3). While cycloheptyl *n*-propylphosphonofluoridate (CHPPF) was only ~3-fold less reactive than the corresponding methylphosphonofluoridate (CHMPF), the cycloheptyl *n*-propylphosphonothiocholine (CHPPT) was found to be 220-fold less reactive than the methylphosphonothiocholine (CHMPT). Since reactivities of the two cycloheptyl methylphosphonates were quite similar (6.8×10^8 and 1.4×10^8 min^{-1} M^{-1} for CHMPF and CHMPT, respectively), the 360-fold lower reactivity of CHPPT, relative to the corresponding fluoridate (CHPPF), may indicate mutual interference of the two bulky phosphonyl substituents. The resemblance of the reactivity ratio between CHPPT and CHMPT (220-fold) and the stereoselectivity observed here toward the VX enantiomers (115-fold; see Table 1) may not be accidental, since the overall dimensions of propyl and ethoxy substituents are quite similar. Therefore, the relative reactivity decrease for both VX^R and propylphosphonothiocholine may originate from similar interactions between the phosphonyl substituents.

The reactivities of HuAChE toward echothiophate and its noncharged isostere nc-echothiophate are also consistent with the idea that the charged bulky leaving group affects the orientation of the ethoxy substituents within the active center. The value of the dissociation constant K_d for the HuAChE−echothiophate Michaelis complex is practically equivalent to that of the corresponding complex with DEFP [2.4×10^{-6} and 1.9×10^{-6} M, respectively (*16*)], despite the fact that in the latter there is no stabilization due to charge interactions. The fact that hydrophobic interactions due to the ethoxy moieties, which stabilize the DEFP complex, do not seem to contribute to accommodation of the echothiophate complex can be understood by assuming that these moieties are improperly oriented with respect to the active center of the enzyme, by interactions within the ligand. Furthermore, removal of the charged interaction, either through modification of the enzyme (aliphatic replacement at position 86 of HuAChE) or by utilizing the noncharged nc-echothiophate, resulted in very low values of the respective bimolecular rate constants k_i (see Table 3). Thus, it appears that irrespective of charge, a large leaving group interferes with the hydrophobic stabilization of the HuAChE−diethyl phosphate complex.

The analysis presented above suggests that comparison of reactivities of the isosteric VX and nc-VX analogues toward HuAChE, in fact, isolates the effect of charge on the relative affinity of the enzyme toward these methylphosphonothiolates. Without the charge interactions and in the absence of a significant contribution of the nc-VX hydrophobic substituents to accommodation in the active center, the reactivities of both nc-VX^S and nc-VX^R enantiomers were exceedingly low, yet the reactivity of HuAChE toward nc-VX^S was still 60-fold higher than that toward nc-VX^R, indicating the presence of specific interactions underlying this HuAChE stereoselectivity. Although such interactions could not be fully characterized on the basis of the functional analysis described here, they appear to be different from those contributing to stereoselectivity toward VX^S. The largest observed effects are related to either introduction or removal of steric obstructions (e.g., effects due to replacement of Gly122 or Tyr337, respectively) rather to the effects related to perturbation at the acyl pocket (see Table 2).

The suggestion that interactions of the charged leaving group constitute the main determinant of HuAChE stereoselectivity toward VX^S may also provide insight into the question regarding the wide range of AChE stereoselectivities toward different methylphosphonates. Namely, the outstanding stereoselectivity toward the P^S-diastereomers of soman [e.g., 7.5×10^4-fold for the P^{S}C^S over the P^{R}C^S diastereomer (*17*)] seems to be in contrast to that observed here, and in previous studies, for VX^S (*40*). The AChE stereoselectivity toward P^{S}C^S- and P^{S}C^R-soman diastereomers is also much higher than the stereoselectivity reported in the past for methylphosphonates carrying other leaving groups such as *p*-nitrophenol (*48*) or thiocholine (*20*, *36*). These different

stereoselectivities result predominantly from the exceedingly low reactivity of the P^R-diastereomers of methylphosphonofluoridates. For instance, while the rate of AChE phosphonylation by VX^S (1.37×10^8 min^{-1} M^{-1}; see Table 1) is similar to those measured for the P^SC^S- and P^SC^R-diastereomers of soman [1.5×10^8 and 0.8×10^8 min^{-1} M^{-1}, respectively (*17*)], the corresponding constant for VX^R (1.18×10^6 min^{-1} M^{-1}) is ~600-fold higher than those for the P^RC^S- or the P^RC^R-soman isomers (2.0×10^3 min^{-1} M^{-1} for both cases). In fact, the reactivities of the P^R-soman diastereomers toward HuAChE resemble those of the nc-VX^S and nc-VX^R enantiomers, suggesting that hydrophobic interactions contribute little to the accommodation of the P^RC^S- or P^RC^R-diastereomer of soman in the AChE active center.

In conclusion, it appears that stereoselectivity of HuAChE toward methylphosphonates is determined by both the nature of the phosphonyl leaving group and the inherent asymmetry of the active center environment. The relative contribution of each of these elements seems to depend on the nature of the specific inhibitor, with the active center asymmetry playing a dominant role in stereoselectivity toward P^S-soman and the positive charge of the leaving group being dominant in stereoselectivity toward VX^S as well as toward other P^S-methylphosphonothiocholines. In contrast to the notion regarding the acyl pocket being the main component of the AChE active center asymmetry, it appears now that other subsites and in particular the PAS contribute to stereoselectivity of HuAChE toward VX and other methylphosphonates.

ACKNOWLEDGMENT

We thank Shirley Lazar, Lea Silberstein, Dana Stein, and Nehama Seliger for their excellent technical assistance and contribution.

SUPPORTING INFORMATION AVAILABLE

Synthesis of 3-(2-bromoethyl)-2,4-dimethylpentane. This material is available free of charge via the Internet at http://pubs.acs.org.

REFERENCES

1. Kaplan, D., Ordentlich, A., Barak, D., Ariel, N., Kronman, C., Velan, B., and Shafferman, A. (2001) Does "butyrylization" of acetylcholinesterase through substitution of the six divergent aromatic amino acids in the active center gorge generate an enzyme mimic of butyrylcholinesterase, *Biochemistry 40*, 7433−7445.
2. Barak, D., Kaplan, D., Ordentlich, A., Ariel, N., Velan, B., and Shafferman, A. (2002) The aromatic "trapping" of the catalytic histidine is essential for efficient catalysis in acetylcholinesterase, *Biochemistry 41*, 8245−8252.
3. Kaplan, D., Barak, D., Ordentlich, A., Kronman, C., Velan, B., and Shafferman, A. (2004) Is aromaticity essential for trapping the catalytic histidine 447 in human acetylcholinesterase, *Biochemistry 43*, 3129−3136.
4. Sussman, J. L., Harel, M., Frolow, F., Oefner, C., Goldman, A., Toker, L., and Silman, I. (1991) Atomic structure of acetylcholinesterase from *Torpedo californica*: a prototypic acetylcholine-binding protein, *Science 253*, 872−879.
5. Bourne, Y., Taylor, P., and Marchot, P. (1995) Acetylcholinesterase inhibition by fasciculin: crystal structure of the complex, *Cell 83*, 503−512.
6. Kryger, G., Harel, M., Giles, K., Toker, L., Velan, B., Lazar, A., Kronman, C., Barak, D., Ariel, N., Shafferman, A., Silman, I., and Sussman, J. L. (2000) Structures of recombinant native and E202Q mutant human acetylcholinesterase complexed with the snake-venom toxin fasciculin-II, *Acta Crystallogr. 56*, 1385−1394.
7. Harel, M., Kryger, G., Rosenberry, T. L., Mallender, W. D., Lewis, T., Fletcher, R. J., Guss, J. M., Silman, I., and Sussman, J. L. (2000) Three-dimensional structures of *Drosophila melanogaster* acetylcholinesterase and of its complexes with two potent inhibitors, *Protein Sci. 9*, 1063−1072.
8. Ordentlich, A., Barak, D., Kronman, C., Flashner, Y., Leitner, M., Segall, Y., Ariel, N., Cohen, S., Velan, B., and Shafferman, A. (1993) Dissection of the human acetylcholinesterase active center determinants of substrate specificity. Identification of residues constituting the anionic site, the hydrophobic site, and the acyl pocket, *J. Biol. Chem. 268*, 17083−17095.
9. Barak, D., Kronman, C., Ordentlich, A., Ariel, N., Bromberg, A., Marcus, D., Lazar, A., Velan, B., and Shafferman, A. (1994) Acetylcholinesterase peripheral anionic site degeneracy conferred by amino acid arrays sharing a common core, *J. Biol. Chem. 264*, 6296−6305.
10. Shafferman, A., Kronman, C., Flashner, Y., Leitner, M., Grosfeld, H., Ordentlich, A., Gozes, Y., Cohen, S., Ariel, N., Barak, D., Harel, M., Silman, I., Sussman, J. L., and Velan, B. (1992) Mutagenesis of human acetylcholinesterase. Identification of residues involved in catalytic activity and in polypeptide folding, *J. Biol. Chem. 267*, 17640−17648.
11. Vellom, D. C., Radic, Z., Li, Y., Pickering, S. N., Camp, A., and Taylor, P. (1993) Amino acid residues controlling acetylcholinesterase and butyrylcholinesterase specificity, *Biochemistry 32*, 12−17.
12. Radic, Z., Gibney, G., Kawamoto, S., MacPhee-Quigley, K., Bongiorno, C., and Taylor, P. (1992) Expression of recombinant acetylcholinesterase in a baculovirus system: kinetic properties of glutamate 199 mutants, *Biochemistry 31*, 9760−9767.
13. Radic, Z., Pickering, N. A., Vellom, D. C., Camp, C., and Taylor, P. (1993) Three distinct domains in the cholinesterase molecule confer selectivity for acetyl- and butyrylcholin-esterase inhibitors, *Biochemistry 32*, 12074−12084.
14. Ariel, N., Ordentlich, A., Barak, D., Bino, T., Velan, B., and Shafferman, A. (1998) The 'aromatic patch' of three proximal residues in the human acetylcholinesterase active centre allows for versatile interaction modes with inhibitors, *Biochem. J. 335*, 95−102.
15. Ordentlich, A., Barak, D., Kronman, C., Ariel, N., Segall, Y., Velan, B., and Shafferman, A. (1998) Functional characteristics of the oxyanion hole in human acetylcholinesterase, *J. Biol. Chem. 273*, 19509−19517.
16. Ordentlich, A., Barak, D., Kronman, C., Ariel, N., Segall, Y., Velan, B., and Shafferman, A. (1996) The architecture of human acetylcholinesterase active center probed by interactions with selected organophosphate, *J. Biol. Chem. 271*, 11953−11962.
17. Ordentlich, A., Barak, D., Kronman, C., Benschop, H. P., De Jong, L. P. A., Ariel, N., Barak, R., Segall, Y., Velan, B., and Shafferman, A. (1999) Exploring the active center of human acetylcholinesterase with stereomers of an organophosphorus inhibitor with two chiral centers, *Biochemistry 38*, 3055−3066.
18. Barak, D., Ordentlich, A., Kaplan, D., Barak, R., Mizrahi, D., Kronman, C., Segall, Y., Velan, B., and Shafferman, A. (2000) Evidence for P−N bond scission in phosphoroamidate nerve agent adducts of human acetylcholinesterase, *Biochemistry 39*, 1156−1161.
19. Hosea, N. A., Berman, H. A., and Taylor, P. (1995) Specificity and orientation of trigonal carboxyl esters and tetrahedral alkylphosphonyl esters in cholinesterases, *Biochemistry 34*, 11528−11536.
20. Hosea, N. A., Radic, Z., Tsigelny, I., Berman, H. A., Quinn, D. M., and Taylor, P. (1996) Aspartate 74 as a primary determinant in acetylcholinesterase governing specificity to cationic organophosphonates, *Biochemistry 35*, 10995−11004.
21. Barak, D., Ariel, N., Velan, B., and Shafferman, A. (1992) Molecular models for human AChE and its phosphonylatiopn products, in *Multidisciplinary Approaches to Cholinesterase Functions* (Shafferman, A., and Velan, B., Eds.) pp 195−199, Plenum Press, London.
22. Shafferman, A., Ordentlich, A., Barak, D., Kronman, C., Ariel, N., and Velan, B. (1998) Contribution of the active center functional architecture to AChE reactivity toward substrates and inhibitors, in *Structure and Function of Cholinesterases and Related Proteins* (Doctor, B. P., Taylor, P., Quinn, D. M., Rotundo, R. L., and Gentry, M., Eds.) pp 203−209, Plenum Press, New York.

23. Kovarik, Z., Radic, Z., Berman, H. A., Simeon-Rudolf, V., Reiner, E., and Taylor, P. (2003) Acetylcholinesterase active centre and gorge conformations analysed by combinatorial mutations and enantiomeric phosphonates, *Biochem. J. 373*, 33−40.
24. Kabachnik, M. I., Brestkin, A. P., Godovkin, N. N., Michelson, M. J., Rozengart, E. V., and Rozengart, V. I. (1970) Hydrophobic areas on the active surface of cholinesterases, *Pharmacol. Rev. 22*, 355−388.
25. Millard, C. B., Koellner, G., Ordentlich, A., Shafferman, A., Silman, I., and Sussman, J. L. (1999) Reaction products of acetylcholinesterase and VX reveal a mobile histidine in the catalytic triad, *J. Am. Chem. Soc. 121*, 9883−9884.
26. Harel, M., Schalk, I., Ehret-Sabatier, L., Bouet, F., Goeldner, M., Hirth, C., Axelsen, P. H., Silman, I., and Sussman, J. L. (1993) Quaternary ligand binding to aromatic residues in the active-site gorge of acetylcholinesterase, *Proc. Natl. Acad. Sci. U.S.A. 90*, 9031−9035.
27. Harel, M., Quinn, D. M., Nair, H. K., Silman, I., and Sussman, J. L. (1996) The X-ray structure of a transition state analog complex reveals the molecular origins of the catalytic power and substrate specificity of acetylcholinesterase, *J. Am. Chem. Soc. 118*, 2340−2346.
28. Soreq, H., Ben-Aziz, R., Prody, C. A., Seidman, S., Gnatt, A., Neville, L., Lieman-Hurwitz, J., Lev-Lehman, E., Ginzberg, D., Lipidot-Lifson, Y., and Zakut, H. (1990) Molecular cloning and construction of the coding region for human acetylcholinesterase reveals a G + C-rich attenuating structure, *Proc. Natl. Acad. Sci. U.S.A. 87*, 9688−9692.
29. Shafferman, A., Velan, B., Ordentlich, A., Kronman, C., Grosfeld, H., Leitner, M., Flashner, Y., Cohen, S., Barak, D., and Ariel, N. (1992) Mutagenesis of human acetylcholinesterase. Identification of residues involved in catalytic activity and in polypeptide folding, *EMBO J. 11*, 3561−3568.
30. Ordentlich, A., Barak, D., Kronman, C., Ariel, N., Segall, Y., Velan, B., and Shafferman, A. (1995) Contribution of aromatic moieties of tyrosine 133 and of the anionic subsite tryptophan 86 to catalytic efficiency and allosteric modulation of acetylcholinesterase, *J. Biol. Chem. 270*, 2082−2091.
31. Barak, D., Ordentlich, A., Bromberg, A., Kronman, C., Marcus, D., Lazar, A., Ariel, N., Velan, B., and Shafferman, A. (1995) Allosteric modulation of acetylcholinesterase activity by peripheral ligands involves a conformational transition of the anionic subsite, *Biochemistry 34*, 15444−15452.
32. Velan, B., Grosfeld, H., Kronman, C., Leitner, M., Gozes, Y., Lazar, A., Flashner, Y., Marcus, D., Cohen, S., and Shafferman, A. (1991) The effect of elimination of intersubunit disulfide bonds on the activity, assembly, and secretion of recombinant human acetylcholinesterase. Expression of acetylcholinesterase Cys-580→Ala mutant, *J. Biol. Chem. 266*, 23977−23984.
33. Kronman, C., Velan, B., Gozes, Y., Leitner, M., Flashner, Y., Lazar, A., Marcus, D., Sery, T., Papier, Y., Grosfeld, H., Cohen, S., and Shafferman, A. (1992) Production and secretion of high levels of recombinant human acetylcholinesterase in cultured cell lines: microheterogeneity of the catalytic subunit, *Gene 121*, 295−304.
34. Ordentlich, A., Kronman, C., Barak, D., Stein, D., Ariel, N., Marcus, D., Velan, B., and Shafferman, A. (1993) Engineering resistance to 'aging' of phosphylated human acetylcholinesterase. Role of hydrogen bond network in the active center, *FEBS Lett. 334*, 215−220.
35. Hall, C. R., Inch, T. D., Inns, R. H., Muir, A. W., Sellers, D. J., and Smith, A. P. (1977) Differences between some biological properties of enantiomers of alkyl S-alkyl methylphosphonothioates, *J. Pharm. Pharmacol. 27*, 574−576.
36. Berman, H. A., and Leonard, K. J. (1989) Chiral reactions of acetylcholinesterase probed with enantiomeric methylphosphonothioates. Noncovalent determinants of enzyme chirality, *J. Biol. Chem. 264*, 3942−3956.
37. Ellman, G. L., Courtney, K. D., Andres, V., and Featherstone, R. M. (1961) A new and rapid colorimetric determination of acetylcholinesterase activity, *Biochem. Pharmacol. 7*, 88−95.
38. Epstein, J., Callahan, J. J., and Bauer, E. (1974) The kinetics and mechanism of hydrolysis of phosphonothiolates in dilute aqueous solution, *Phosphorus 4*, 157−163.
39. Hart, G. J., and O'Brien, R. D. (1973) Recording spectrophotometric method for determination of dissociation and phosphorylation constants for the inhibition of acetylcholinesterase by organophosphates in the presence of substrate, *Biochemistry 12*, 2940−2945.
40. Benschop, H. P., and De Jong, L. P. A. (1988) Nerve agent stereoisomers: analysis, isolation and toxicology, *Acc. Chem. Res. 21*, 368−374.
41. Greenblatt, H. M., Kryger, G., Lewis, T., Silman, I., and Sussman, J. L. (1999) Structure of acetylcholinesterase complexed with (−)-galanthamine at 2.3 Å resolution, *FEBS Lett. 463*, 321−326.
42. Albaret, C., Lacoutiere, S., Ashman, W. P., Groment, D., and Fortier, P.-L. (1997) Molecular mechanics study of nerve agent O-ethyl S-[2-(diisopropylamino)ethyl]-methylphosphonothioate (VX) bound to the active site of *Torpedo californica* acetylcholinesterase, *Proteins 28*, 543−555.
43. Jarv, J. (1984) Stereochemical aspects of cholinesterase catalysis, *Bioorg. Chem. 12*, 259−278.
44. Harel, M., Sussman, J. L., Krejci, E., Bon, S., Chanal, P., Massoulie, J., and Silman, I. (1992) Conversion of acetylcholinesterase to butyrylcholinesterase: modeling and mutagenesis, *Proc. Natl. Acad. Sci. U.S.A. 89*, 10827−10831.
45. Boter, H. L., De Jong, L. P. A., and Kienhuis, H. (1971) in *Interaction of Chemical Agents with Cholinergic Mechanisms*, Israel Institute of Biological Research 16th Annual Biology Conference, pp 9−26, Israel Institute of Biological Research, Tel Aviv, Israel.
46. Levy, D., and Ashani, Y. (1986) Synthesis and in vitro properties of a powerful quaternary methylphosphonate inhibitor of acetylcholinesterase. A new marker in blood-brain barrier research, *Biochem. Pharmacol. 35*, 1079−1085.
47. Berman, H. (1995) Reaction of acetylcholinesterase with organophosphonates, in *Enzymes of the Cholinesterase Family* (Quinn, D. M., Balasubramanian, A. S., Doctor, B. P., and Taylor, P., Eds.) pp 177−182, Plenum Press, New York.
48. Benschop, H. P., Konings, C. A. G., Van Gendern, J., and De Jong, L. P. A. (1985) Stabilization and gas chromatographic analysis of the four stereoisomers of 1,2,2-trimethylpropyl methylphosphonofluoridate (soman) in rat blood, *Anal. Biochem. 151*, 242−253.
49. Van der Schans, M. J., Lander, B. J., van der Wiel, H., Langenberg, J. P., and Benschop, H. P. (2003) Toxicokinetics of the nerve agent (±)-VX in anesthetized and atropinized hairless guinea pigs and marmosets after intravenous and percutaneous administration, *Toxicol. Appl. Pharmacol. 191*, 48−62.
50. Massoulie, J., Sussman, J. L., Doctor, B. P., Soreq, H., Velan, B., Cygler, M., Rotundo, R., Shafferman, A., Silman, I., and Taylor, P. (1992) Recommendations for nomenclature in cholinesterases, in *Multidisciplinary Approaches to Cholinesterase Functions* (Shafferman, A., and Velan, B., Eds.) pp 285−288, Plenum Press, New York.

BI0490946